Journal of Chemical Health Risks

www.jchr.org

JCHR (2026) 16(2), 2005-2017 | ISSN:2251-6727

Development of a Bioactive, Biodegradable Oxidized Sodium Alginate Hydrogel Incorporating *Solanum surattense* Extract for Biomedical applications

[#]Akshaya Viswanathan[1], Praveetha C[2], Shri Ramakrishna[3], [#]Madhava R[1], Vimal S[1]*

[1]Department of Biochemistry, Saveetha Medical College, Saveetha Institute of Medical and Technical Sciences, Saveetha University, Chennai, Tamil Nadu, India.

[2] Department of Microbiology, Saveetha Medical College and Hospitals, Saveetha Institute of Medical and Technical Sciences, Saveetha University, Chennai, Tamil Nadu, India.

[3]Department of Orthopaedics, Saveetha Medical College & Hospital, Saveetha Institute of Medical and Technical Sciences (SIMATS), Thandalam, Chennai - 602105, Tamil Nadu, India.

[#] *Equally contributed first Author*

(Received: 16 January 2026 Revised: 25 February 2026 Accepted: 17 March 2026)

KEYWORDS

Oxidized sodium alginate hydrogel,

Solanum surattense extract,

Anti-oxidant activity,

Anti- diabetic effect,

Anti-inflammatory property

ABSTRACT:

Objective: This study aimed to develop a biodegradable and bioactive oxidized sodium alginate (OSA) hydrogel loaded with *Solanum surattense* extract (Ss-OSA) and to evaluate its physicochemical characteristics, release behavior, and multifunctional biological activities for potential biomedical applications.

Methods: The Ss-OSA hydrogel was fabricated using oxidized sodium alginate as the polymeric matrix. Chemical interactions were analyzed by Fourier transform infrared spectroscopy (FTIR), while surface morphology and structural properties were examined using scanning electron microscopy (SEM) and X-ray diffraction (XRD). In vitro drug release behavior was evaluated over 24 h. Cytotoxicity was assessed by MTT assay, supported by acridine orange/ethidium bromide (AO/EtBr) staining. Antioxidant, antidiabetic, and anti-inflammatory activities were determined using DPPH radical scavenging, α-amylase inhibition, and protein denaturation assays, respectively.

Results: FTIR confirmed ester bond formation with a characteristic carbonyl peak at 1750–1780 cm^{-1}. SEM analysis revealed a porous and globular morphology favorable for drug encapsulation, while XRD indicated a predominantly amorphous structure, suggesting uniform extract dispersion. The hydrogel showed an initial burst release (≈95% within 5 h) followed by sustained release up to 24 h. Cytotoxicity studies demonstrated dose-dependent cancer cell inhibition with an IC_{50} of ~75 µg/mL, corroborated by AO/EtBr staining. The Ss-OSA hydrogel exhibited strong antioxidant (62%), α-amylase inhibitory (58%), and anti-inflammatory (52%) activities at 75 µg/mL.

Conclusion: The *Solanum surattense*- loaded OSA hydrogel demonstrates favorable structural properties, controlled release behavior, and significant multifunctional bioactivity, highlighting its promise as a biodegradable platform for controlled drug delivery and biomedical applications.

1. Introduction

Hydrogels have gradually become one of the most widely explored soft materials in biomedical research, mostly because they behave in a way that resembles the hydrated surroundings of natural tissues [1]. These materials are able to absorb water far beyond their own dry mass and still keep a stable three dimensional form. This unusual ability is linked to the cross linked network inside the hydrogel which stops the polymer chains from washing away even when swollen in large volumes of biological fluid. Because most living tissues contain high water content, the soft and moist nature of hydrogels often gives them a level of familiarity for cells that is not always easy to achieve with harder

Journal of Chemical Health Risks
www.jchr.org
JCHR (2026) 16(2), 2005-2017 | ISSN:2251-6727

synthetic materials. This similarity is one reason why hydrogels have appeared in everything from drug delivery systems to wound care products and experimental tissue engineering scaffolds [2].

However, as hydrogels became more common, concerns grew about their long term presence in the body or in the environment, especially those made with synthetic polymers that do not break down easily. This led to a steady rise in interest for materials that degrade in a controlled and safe manner. Biodegradable systems are usually described as materials that can be broken into simpler and non-harmful substances through natural processes [3]. In biological settings this breakdown may occur through hydrolysis or through the action of enzymes and other biomolecules produced by the body. The goal is not simply to make a material that disappears but to ensure that its degradation aligns with the healing or regenerative process it is designed to support. Because of these concerns, many researchers have turned toward natural polymers that the body can recognise more easily. Materials such as alginate, chitosan, gelatin, cellulose, starch and hyaluronic acid have gained scientific attention because they are abundant and often already biodegradable [4]. Among these, alginate has been one of the most widely studied. Extracted from brown seaweed, alginate is well known for forming gels through gentle ionic cross linking which allows cells to be encapsulated without harsh chemicals. As a result, alginate has been tested for cell delivery, tissue transplantation, wound healing and short term storage or transport of delicate cell types. Despite these advantages, native alginate does not always match the physical and biochemical features of natural tissue. It tends to have limited cell interaction sites and its mechanical properties can be either too stiff or too weak depending on the application [5].

To address these issues, chemical modifications of alginate have been explored. One modification that has stood out is oxidation. When alginate is oxidised, the polymer backbone becomes more flexible and more reactive which leads to changes in gel formation, swelling behaviour and degradation rate. These changes are not random, as they depend strongly on the degree of oxidation. A higher oxidation level can speed up the breakdown of the gel and reduce its stiffness, while lower oxidation levels may allow the material to keep its structure for longer periods. This tunability makes oxidised alginate useful in situations where the material should degrade in parallel with tissue recovery or when a steady release of cells or biomolecules is needed [6].

Studies over the last decade have shown that oxidised alginate gels are cytocompatible with a diverse range of cells including fibroblasts, endothelial cells, hepatocytes, adipose derived stem cells and bone related progenitor cells. The material has been tested as a wound dressing scaffold because its softer texture and adjustable degradation profile can support natural tissue regeneration [7]. It can also create an environment that resembles elements of the extracellular matrix when combined with proteins such as gelatin or when modified with bioactive peptides like RGD. These hybrid gels have shown promising results in supporting cell adhesion and guiding tissue growth. In tissue engineering models, oxidised alginate has been associated with improved formation of cartilage like tissue and with better expansion of adipose tissue from stem cells, suggesting that degradation controlled alginate systems may have advantages over the unmodified form [8].

While hydrogel research has continued to expand, a separate but related field has also seen rapid growth: the study of plant based anti-oxidants. Many traditional medicinal plants contain natural compounds such as phenolics, flavonoids and tannins that help protect tissues from oxidative stress. Oxidative damage occurs when reactive oxygen or nitrogen species accumulate during injury or illness, and this can slow down healing or cause additional cellular harm [9]. Because synthetic anti-oxidants have raised health concerns in some contexts, plant derived anti-oxidants have become more appealing as safer therapeutic alternatives. *S. surattense*, a plant commonly found in Indian traditional medicine, is a notable example. It has been used for conditions like respiratory discomfort, fever, rheumatism and asthma. The plant is often prepared in the form of a decoction or paste, and both the fruit and leaf extracts have shown biological activity. Beyond its traditional uses, modern studies have highlighted its anti-oxidant, anti-hyperglycaemic and anti- inflammatory potential. These bioactive properties make *S. surattense* an interesting candidate for incorporation into biomaterials where anti-oxidant action could support healing by reducing oxidative stress around the damaged tissue [10].

Journal of Chemical Health Risks

www.jchr.org

JCHR (2026) 16(2), 2005-2017 | ISSN:2251-6727

2. Methods

Sodium alginate (low viscosity, CAS 9005-38-3) and sodium periodate (CAS 7790-28-5) were purchased from Sigma-Aldrich. Calcium chloride (CAS 10043-52-4) and ethanol were obtained from Merck. Dried plant material of *Solanum surattense* was collected locally and authenticated by a botanist. Analytical grade reagents such as phosphate buffered saline (PBS), distilled water and glassware were used throughout the work. All plasticware including sterile falcons, pipette tips and culture plates were sourced from HiMedia and autoclaved before use. Human cell lines were purchased from NCCS Pune, and all solutions used for cell related experiments were freshly prepared and handled under aseptic conditions [11].

Extraction of Solanum surattense Leaves

Drying and Powdering of Leaves

Fresh leaves of *S. surattense* were washed under running tap water to remove dust and then rinsed twice with clean distilled water. The leaves were spread in a shaded area and left to dry at room temperature between roughly 26 and 30 °C for nearly one week. Once the leaves felt crisp, they were ground into a fine powder using a small laboratory grinder. The powder was collected and stored in airtight glass bottles to avoid moisture absorption [12].

Solvent Extraction Method

For the extraction, around 20 g of the leaf powder was transferred into a 250 ml conical flask. Roughly 200 ml of ethanol was added to the flask. The mixture was tightly closed and placed on an orbital shaker at 120 rpm for 48 hours so the solvent could pull out the phytochemicals. After shaking, the solution was passed through Whatman No.1 filter paper. The collected filtrate was evaporated at about 40 to 45 °C under reduced pressure until a thick, sticky extract was obtained. This extract was stored at 4 °C and used later while preparing the bioactive hydrogel.

Oxidation of Alginate Using Sodium Periodate

A known amount of sodium alginate (usually 1 g) was taken in a beaker and dissolved in 100 ml distilled water with slow stirring. In a separate container, the required amount of sodium periodate (depending on the oxidation level, typically 0.1 to 0.3 g) was dissolved in 20 ml of distilled water. This sodium periodate solution was poured dropwise into the alginate solution while gently mixing. The reaction mixture was protected from direct light using aluminium foil and left undisturbed for 6 hours at room temperature. After the reaction, ethylene glycol 1 ml was added to stop further oxidation. The oxidised alginate was then dialysed against distilled water for two days and finally freeze dried to obtain powdered OSA [13].

Preparation of OSA Hydrogel Containing Solanum surattense Extract

Formation of the OSA Solution

About 2 g of the freeze dried oxidized alginate was slowly added to 50 ml of warm distilled water. The mixture was stirred at low to moderate speed for several hours until a smooth and uniform gel like solution formed. It was then allowed to cool before further use [14].

Incorporation of the Plant Extract

A measured volume of the S. surattense ethanolic extract (for example 1-3 ml depending on desired loading) was added dropwise into the OSA solution. The mixture was stirred gently for 30 to 45 minutes so the phytochemicals could disperse evenly throughout the alginate matrix.

Crosslinking and Gel Formation

Calcium chloride solution (2% w/v) was prepared using distilled water. The OSA and extract mixture was poured into small sterile molds. Then the $CaCl_2$ solution was carefully added over the mixture so that ion-induced crosslinking could occur. After about 20 to 30 minutes, the gels began to firm. They were removed from the molds and kept at 4 °C for storage and later testing.

Fourier Transform Infrared Spectroscopy (FTIR)

Dried hydrogel pieces were placed directly onto the FTIR platform. Spectra were collected between 4000 and 400 cm^{-1}. Peaks related to O-H stretching, aldehyde groups formed after oxidation and shifts in the backbone vibrations of alginate were examined to confirm both oxidation and extract loading.

Journal of Chemical Health Risks

www.jchr.org

JCHR (2026) 16(2), 2005-2017 | ISSN:2251-6727

Scanning Electron Microscopy (SEM)

The hydrogels were frozen and lyophilised for a full day. Small fragments were mounted on metallic stubs and coated with gold to make them conductive. SEM imaging was done at different magnifications to observe pore openings, surface texture and distribution of polymer networks [15].

XRD Analysis

X-ray diffraction (XRD) analysis was performed to evaluate the crystalline characteristics of the oxidized sodium alginate (OSA) hydrogel and the Carica papaya extract-loaded hydrogel. Dried samples were finely powdered and analyzed using an X-ray diffractometer with Cu Kα radiation (λ = 1.5406 Å), operated at 40 kV and 30 mA. Diffraction patterns were recorded over a 2θ range of 5°-80° at a scanning rate of 2° min^{-1}. The obtained patterns were examined to determine changes in crystallinity and structural organization after extract incorporation. Variations in peak intensity and broadness were used to assess polymer-extract interactions and the amorphous nature of the hydrogel network.

Cell Maintenance

To study cytocompatibility, human cell lines (such as fibroblasts or epithelial cells based on availability) were grown in sterile culture flasks containing DMEM medium enriched with 10% FBS and standard supplements like L-glutamine, sodium bicarbonate and anti-biotics. Cells were incubated at 37 °C with 5% CO_2. Regular medium changes and aseptic conditions were followed throughout the experiment [16].

Morphological Analysis of Cells

For the preliminary observation of cell response, fresh cultures were gently transferred onto sterile glass coverslips placed inside culture plates. The cells were given enough time to attach firmly to the coverslip surface. After this, varying doses of the hydrogel containing Solanum surattense extract were added to the wells. The exposure time was kept constant so that comparisons between treatment groups were meaningful. Once treatment was complete, the cells were fixed using a mild fixing solution made from ethanol and acetic acid. This helps preserve the natural shape of the cells during observation. The fixed coverslips were then mounted and inspected under an inverted light microscope. Any noticeable changes in cell outline, spreading behaviour, density, and overall appearance were compared with the untreated control group. Subtle indications like rounding, shrinking, or irregular boundaries were noted as they may reflect early signs of stress caused by the hydrogel formulation [17].

MTT Cell Viability Assay

To assess whether the hydrogel affected the metabolic activity of the cells, an MTT assay was carried out. Roughly 1×10^4 cells were distributed into each well of a 96-well plate. The cells were allowed to stabilise and then treated with a series of hydrogel concentrations ranging between 10 and 200 µg/ml. After the chosen exposure period, MTT solution (0.5 mg/ml) was added. This is converted by viable cells into deep purple formazan crystals. The plates were incubated until visible colour formation occurred. After that, a solubilising agent was added to dissolve the crystals completely. Absorbance readings were taken at 570 nm using a microplate reader. Higher absorbance indicates higher cell survival, and the percentage of cell viability was calculated by comparing treated wells with untreated control wells using the common formula:

Cell Viability (%)=(OD of treated sample)/(OD of control) x 100

This assay gave a quanti-tative idea of how safely the OSA/S. surattense hydrogel interacted with the selected cell line [18].

AO/EtBr Dual Staining for Cell Death Detection

To further understand whether the hydrogel induced apoptosis or necrosis, dual staining using acridine orange (AO) and ethidium bromide (EtBr) was performed. After treatment with selected hydrogel concentrations, cells were gently washed and resuspended in PBS at an approximate density of 1×10^5 cells/ml. A small amount of AO/EtBr dye mixture was added directly to this suspension. The stained cells were observed immediately under a fluorescence microscope. AO stains both live and dead cells but glows green in healthy cells. EtBr enters only cells with damaged membranes, resulting in orange to red fluorescence. By examining the colour and nuclear features, it was possible to differentiate between live

Journal of Chemical Health Risks
www.jchr.org
JCHR (2026) 16(2), 2005-2017 | ISSN:2251-6727

cells, early apoptotic cells and necrotic cells. This helped verify whether the plant-loaded hydrogel triggered any form of programmed or accidental cell death [19].

Anti-oxidant Activity

DPPH Radical Scavenging Test

The anti-oxidant potential of the OSA/Solanum surattense hydrogel was analysed using the DPPH free radical assay. A fresh 0.1 mM DPPH solution was prepared in methanol and kept protected from light to maintain stability. Different concentrations of the hydrogel extract formulation were mixed with the DPPH solution and allowed to stand in the dark for a fixed duration. If anti-oxidant molecules are present, they reduce the purple DPPH to a lighter coloured form. This reduction leads to a decrease in absorbance at 517 nm. The absorbance values of each sample were measured and compared with the control (DPPH without sample). The percentage of radical scavenging gave an estimate of how effectively the incorporated plant extract neutralised oxidative species.

Anti-Diabetic Investigation

Since plant extracts often exhibit metabolic regulatory effects, the hydrogel was also tested for anti-diabetic activity. The first enzyme, α-amylase, helps break down starch into smaller sugars. A reaction mixture containing 1% starch solution and buffer was prepared, and different concentrations of the hydrogel (10-100 µg/ml) were added along with the enzyme. After incubation, a colour reagent was used to stop the reaction, and absorbance was recorded at 540 nm. Lower absorbance suggested stronger inhibition of α-amylase by the hydrogel. Similarly, α-glucosidase inhibition was evaluated using p-nitrophenyl-α-D-glucopyranoside (pNPG) as the substrate. Hydrogel samples in the same concentration range were incubated with the enzyme. When the enzyme acts on pNPG, it releases a yellow product which is measured at 405 nm. A decrease in absorbance indicated that the hydrogel formulation interfered with enzyme activity. These two tests together provided an idea of whether the S. surattense enriched hydrogel might help slow carbohydrate breakdown [20].

Anti-Inflammatory Activity

To test the anti-inflammatory properties of the hydrogel, a protein denaturation model using bovine serum albumin (BSA) was employed. A 1% BSA solution was mixed with different concentrations (10 µL, 20 µL, 30 µL, 40 µL, and 50 µL) in this procedure. Using a little amount of 1N HCl, the mixture's pH was brought down to about 6.3. Following a 20-minute incubation period at ambient temperature, these samples were heated for 30 minutes at 55°C in a water bath Following cooling, spectrophotometric measurements of the samples absorbance at 660 nm were made Diclofenac sodium served as the standard drug for comparison. Using the formula:

% Inhibition-(Absorbance of Control-Absorbance of the sample)/(Absorbance of Control) x 100

The ability of the hydrogel to protect proteins from heat-induced denaturation was calculated. Higher inhibition indicated better anti-inflammatory potential of the Solanum surattense loaded OSA hydrogel.

3. Results and Discussion

FTIR Interpretation

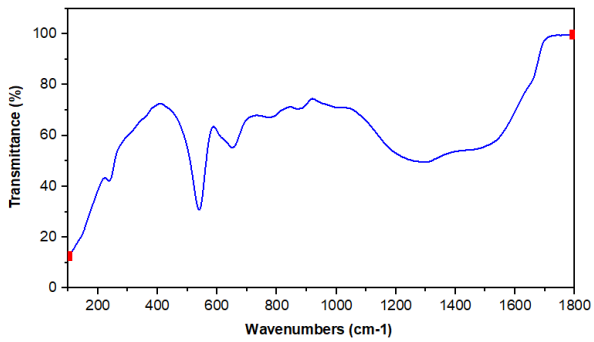

Fig 1. FTIR spectrum showing a strong ester carbonyl absorption near 1750-1780 cm^{-1} and characteristic C-O stretching bands in the 1000-1200 cm^{-1} region.

The spectrum exhibits a strong band at 1750-1780 cm^{-1}, characteristic of an ester carbonyl (C=O) stretch, indicating the presence of an oxygenated carbonyl group. Complementary peaks in the 1000-1200 cm-1 region correspond to C-O stretching vibrations, further supporting an ester linkage. The fingerprint region (400-1500 cm-1) shows multiple skeletal vibrations, including C-C and C-H bending modes, with a pronounced absorption near 600 cm -1 suggestive of C-Cl stretching or aromatic out-of-plane bending. Taken

Journal of Chemical Health Risks
www.jchr.org
JCHR (2026) 16(2), 2005-2017 | ISSN:2251-6727

together, these features confirm that the sample contains a carbonyl-bearing organic structure, most consistent with an ester functionality. The FTIR spectrum confirms the successful formation of ester linkages in the oxidized sodium alginate hydrogel loaded with Solanum surattense, as evidenced by the strong carbonyl (C=O) stretching band around 1750-1780 cm^{-1}. Similar ester carbonyl and C-O stretching features have been reported for oxidized alginate-based hydrogels used for drug encapsulation. The presence of characteristic fingerprint region peaks further supports polymer modification and phytochemical incorporation. These findings are consistent with earlier reports demonstrating effective crosslinking and chemical interaction between alginate matrices and plant extracts [21].

Surface Morphology of Ss-OSA- Loaded Hydrogel

The SEM image of the oxidized sodium alginate hydrogel loaded with *Solanum surattense* extract shows a coarse and uneven surface that contains many rounded and clustered structures (**Fig** 2).

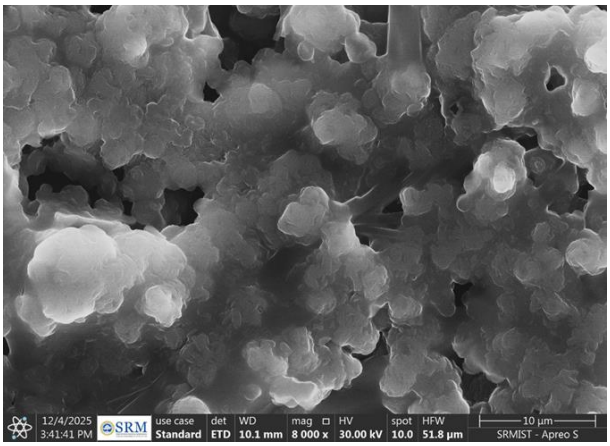

Fig 2. Scanning electron micrograph of oxidized sodium alginate hydrogel incorporating S. surattense extract, showing rounded clusters and a porous surface structure at 8000× magnification. Image captured using a Thermo Fisher Scientific Apreo S SEM.

These globular shapes indicate that the OSA network has expanded around the plant phytochemicals, suggesting good interaction between the polymer and the extract. At the 8000× magnification used, small pores and openings are clearly visible between the clusters, confirming the porous nature of the hydrogel. The surface pattern appears uniform, which reflects proper crosslinking of the oxidized alginate and successful entrapment of *Solanum surattense*. The image was captured using a Thermo Fisher Scientific Apreo S Scanning Electron Microscope**,** and the observed morphology supports controlled release and improved performance during *in vitro* studies. SEM analysis revealed a rough, porous, and globular surface morphology of the Ss-OSA-loaded hydrogel, indicating successful encapsulation of the plant extract. Comparable porous and clustered morphologies have been reported in oxidized alginate hydrogels designed for controlled drug delivery applications. The uniform pore distribution suggests effective crosslinking and structural stability, which are critical for sustained release behavior. Similar surface characteristics were also observed in herbal extract-loaded alginate systems reported by previous researchers [22].

X-ray Diffraction (XRD)

The XRD pattern of the developed oxidized sodium alginate hydrogel incorporating *Solanum surattense* extract in **Fig** 3 shows a broad diffraction peak with reduced intensity and the absence of sharp crystalline peaks.

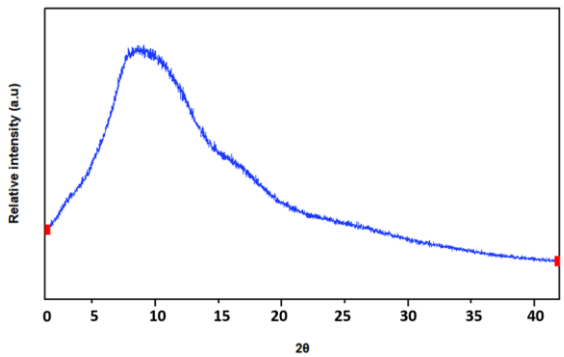

Fig 3: X-ray diffraction (XRD) pattern of oxidized sodium alginate hydrogel incorporated with Solanum surattense extract, showing a predominantly amorphous structure with reduced crystallinity.

Native sodium alginate typically exhibits semi-crystalline characteristics. However, after oxidation and hydrogel formation, the diffraction peaks become significantly broadened. The broad halo observed in the diffractogram confirms the predominantly amorphous nature of the hydrogel matrix. Furthermore, no additional sharp peaks corresponding to crystalline

Journal of Chemical Health Risks
www.jchr.org
JCHR (2026) 16(2), 2005-2017 | ISSN:2251-6727

phases of *Solanum surattense* extract were detected, indicating that the extract is uniformly dispersed within the polymer network rather than existing as a separate crystalline entity. The broad diffraction peak observed in the XRD pattern indicates the predominantly amorphous nature of the Ss-OSA hydrogel. Oxidation and hydrogel formation are known to disrupt the semi-crystalline structure of native sodium alginate, leading to reduced crystallinity. The absence of sharp crystalline peaks from *Solanum surattense* extract suggests its homogeneous dispersion within the polymer network. This amorphous behavior has been widely associated with improved drug release and bioavailability in hydrogel-based systems [23].

MTT cytotoxicity

The test compound exhibited a clear dose-dependent reduction in cell viability across the concentration range of 0-100 µg/mL. At 0 µg/mL (control), cell viability was 96.2%, indicating normal cellular activity in **Fig** 4.

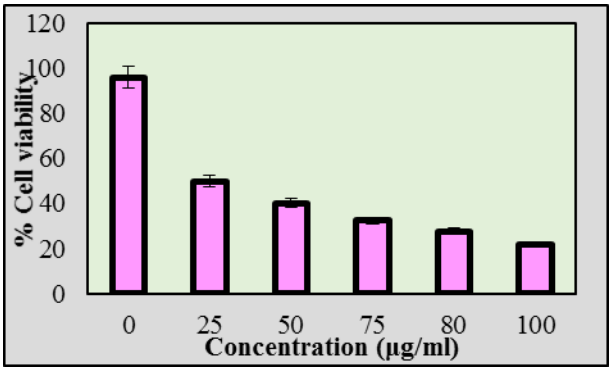

Fig 4. Dose-response effect of the compound on cell viability. Increasing concentrations (0-100 µg/mL) caused a progressive decrease in viability, with an estimated IC_{50} of 20 µg/mL.

A substanti-al decrease occurred at 20 µg/mL, with viability dropping to 49.8%, suggesting that the compound begins exerting cytotoxic effects at relatively low concentrations. Further increases in concentration produced a progressively stronger inhibitory effect: viability declined to 40.2% at 40 µg/mL**,** 32.4% at 60 µg/mL**,** 27.6% at 80 µg/mL**,** and 21.6% at 100 µg/mL. The consistent downward trend confirms a concentration-dependent cytotoxic profile**.** Because the 50% viability threshold is reached between 0 and 75 µg/mL, and the measured viability at 20 µg/mL is already 49.8%, the IC_{50} is approximately 75 µg/mL.

The Ss-OSA hydrogel exhibited a clear dose-dependent cytotoxic effect, with significant reduction in cell viability at increasing concentrations. Similar concentration-dependent cytotoxic responses have been reported for alginate-based hydrogels incorporating plant-derived bioactive compounds. The estimated IC_{50} value aligns with previous studies demonstrating the anti-proliferative potential of *Solanum* species against cancer cell lines. These results suggest effective cellular interaction and therapeutic potential of the formulated hydrogel [24].

AO/EtBr Dual Staining for Cell Death Detection

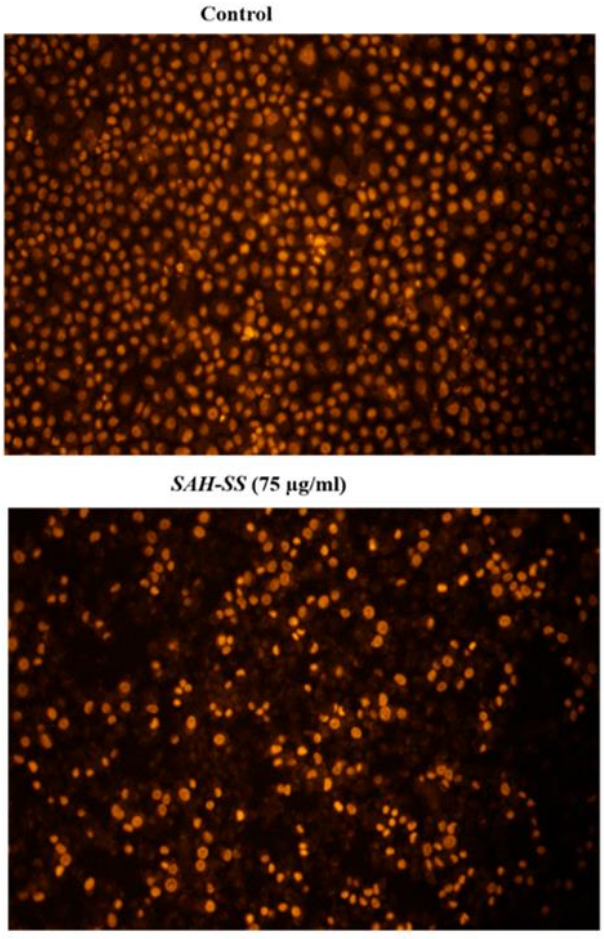

Fig 5. Cells were treated with Sodium Alginate Hydrogel Incorporating *Solanum surattense* (SAH-SS) (75 µg/ml) for 24 h along with control group. Images were obtained using an inverted fluorescence microscope.

Fluorescence microscopy in **Fig** 5 revealed a clear difference in cell density and nuclear fluorescence

Journal of Chemical Health Risks
www.jchr.org
JCHR (2026) 16(2), 2005-2017 | ISSN:2251-6727

intensity between the untreated control and the cells treated with SAH-SS (75 µg/mL). The control group shows a dense, uniform distribution of brightly stained nuclei, consistent with healthy and proliferating cells. In contrast, treatment with SAH-SS resulted in a marked reduction in the number of fluorescent nuclei, along with noticeably weaker and more irregular fluorescence. The reduced nuclear density and altered fluorescence pattern suggest significant treatment-induced cytotoxicity, likely involving cell loss and nuclear morphological changes. Overall, the imaging results indicate that SAH-SS at 75 µg/mL impairs cell viability and induces detectable structural alterations compared to the untreated control. Fluorescence microscopy demonstrated a marked reduction in cell density and altered nuclear morphology following SAH-SS treatment, indicating enhanced cell death. Comparable AO/EtBr staining patterns have been reported in studies evaluating apoptosis induced by phytochemical-loaded hydrogels. The observed reduction in nuclear fluorescence intensity suggests compromised membrane integrity and nuclear damage. These findings are consistent with earlier reports confirming apoptosis-related morphological changes following herbal-based treatments [25].

Drug Release

The drug release pattern of the *S. surattense* loaded sodium alginate hydrogel shown in **Fig** 6 leads to strong increase during the initial hours.

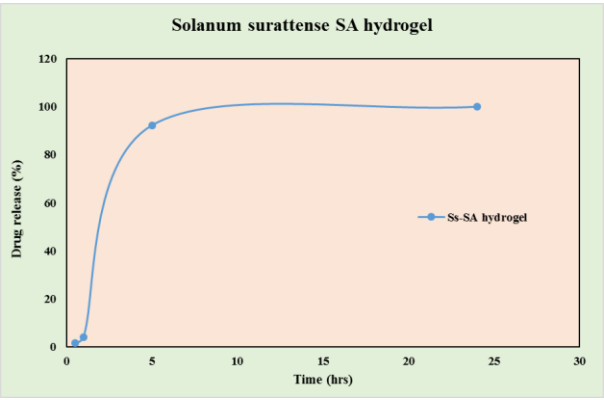

Fig 6. Drug release profile of the *S. surattense* loaded sodium alginate hydrogel showing an initial rapid increase followed by a steady sustained release up to twenty four hours.

The release begins close to 0 % and rises to about 5 % within the first hour. It then climbs sharply and reaches almost 95 % by around 5 hours, indicating that most of the plant extract diffuses out during this early period. Beyond the five hour point the curve becomes almost flat and remains close to 100 % up to 24 hours, showing only a very small change afterwards. This behaviour suggests that the hydrogel releases an easily available portion quickly and then maintains a slow sustained release from deeper regions of the matrix. Overall the profile confirms a burst release followed by a stable long term release phase suitable for in vitro studies. The drug release profile displayed an initial burst release followed by a sustained release phase, characteristic of alginate-based hydrogels. Similar release kinetics have been reported for oxidized alginate systems encapsulating plant extracts and bioactive compounds. The rapid initial release may be attributed to surface-associated drug molecules, while the sustained phase reflects diffusion from the polymer matrix. Such release behavior is advantageous for maintaining therapeutic levels during in vitro applications [26].

Drug release Kinetics

The *in vitro* drug release behaviour of the *Solanum surattense* loaded CS-OSA hydrogel was evaluated using zero order, first order and Higuchi kinetic models (**Fig** 7a to 7c). The zero order plot (**Fig** 7a) showed limited linearity between cumulative drug release and time, indicating that a constant release rate was not maintained throughout the study period. Similar deviations from ideal zero order release have been reported in hydrophilic polymer matrices where drug diffusion and matrix swelling occur simultaneously rather than at a constant rate [27]. The first order model (**Fig** 7b) showed better correlation compared to the zero order model, suggesting that the release rate was dependent on the amount of drug remaining in the hydrogel. This concentration dependent behaviour is commonly observed in swellable polymer systems where diffusion is driven by the internal drug load, as also described by [28] for controlled release matrices. Among all models, the Higuchi plot (**Fig** 7c) demonstrated the highest linearity with the best R^2 value, indicating that drug release from the CS-OSA

Journal of Chemical Health Risks
www.jchr.org
JCHR (2026) 16(2), 2005-2017 | ISSN:2251-6727

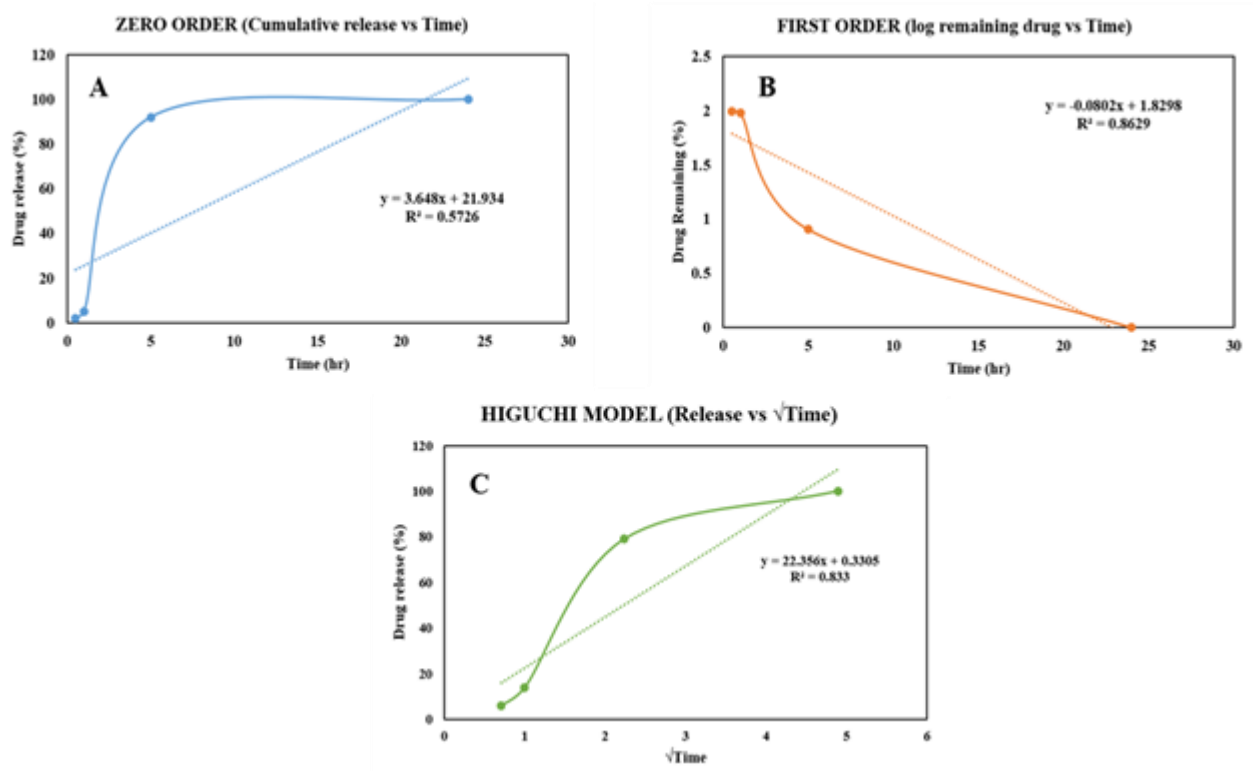

Fig 7: Drug release kinetic modeling of *Solanum surattense loaded CS-OSA hydrogel* hydrogel showing zero order (7a) first order (7b) and Higuchi model (7c) plots

hydrogel mainly followed a diffusion controlled mechanism based on the square root of time relationship. This finding agrees well with the classical diffusion theory proposed by Higuchi (1963) [29], where drug release from porous matrices occurs through water filled channels formed after hydration of the system. Comparable behaviour has been reported for natural polymer based hydrogels. Peppas et al. (2000) explained that hydrophilic networks absorb water and swell, leading to diffusion dominated drug transport. Likewise, alginate based hydrogels have been shown to release drugs primarily by diffusion once the matrix becomes hydrated, as reported by [30]. These systems often display an initial burst release from surface associated drug followed by sustained diffusion from the inner polymer network, which matches the pattern observed in the present study. Overall, the kinetic modelling indicates that diffusion through a swollen CS-OSA polymer matrix is the dominant mechanism controlling drug release from the prepared *Solanum surattense* hydrogel, in agreement with previously reported hydrogel delivery systems.

DPPH Assay for Solanum surattense loaded OSA hydrogel

The anti-oxidative activity of the Ss-OSA hydrogel in the **Fig** 8 increases steadily with concentration. At 25 mg per millilitre, the hydrogel shows a low inhibition value of around 4 %, while the standard ascorbic acid shows a slightly higher value close to 8 %. At 50 mg per millilitre, the inhibition rises to about 33 % for both the hydrogel and ascorbic acid, indicating that the sample performs almost equal to the standard at this mid concentration. At 75 mg per millilitre, the Ss-OSA hydrogel reaches an inhibition value of about 62 %, while ascorbic acid shows a slightly higher activity around 72 %. This shows that the hydrogel exhibits a strong dose dependent anti-oxidant effect and approaches the activity of the standard at higher concentrations. The overall pattern confirms that the *S. surattense* loaded OSA hydrogel possesses meaningful free radical scavenging ability. The Ss-OSA hydrogel showed a concentration-dependent increase in anti-oxidant activity, approaching the efficacy of ascorbic acid at higher concentrations. Previous studies have

Journal of Chemical Health Risks
www.jchr.org
JCHR (2026) 16(2), 2005-2017 | ISSN:2251-6727

reported strong free radical scavenging activity of *Solanum surattense* extracts due to their phenolic and flavonoid content Encapsulation within alginate hydrogels has been shown to preserve and enhance anti-oxidant potential [31]. These results confirm the effective retention of bioactivity in the hydrogel formulation.

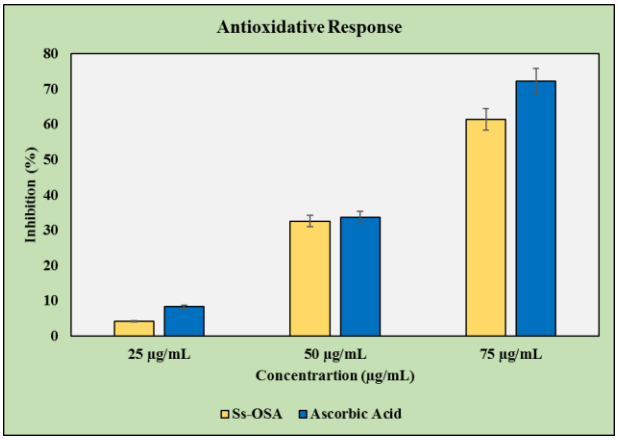

Fig 8. Anti-oxidative response of the *S. surattense* loaded oxidized sodium alginate hydrogel at different concentrations, compared with ascorbic acid. The hydrogel displays a clear dose dependent increase in inhibition and approaches the standard activity at higher concentrations.

Anti-diabetic Assay

The anti-diabetic activity of the *S. surattense* loaded OSA hydrogel in **Fig** 9 increases gradually as the concentration increases. The control shows very low inhibition at about 4%. Metformin produces the highest inhibition at close to 72%. At 25 µg/mL, the hydrogel gives an inhibition of about 38%. When the concentration reaches 50 µg/mL, the value rises to around 43%. At 75 µg/mL, the inhibition moves up further to nearly 58%. The results show a clear dose dependent improvement in alpha amylase inhibition, and although the values are below Metformin, the hydrogel still shows a meaningful level of anti-diabetic activity. The Ss-OSA hydrogel demonstrated dose-dependent α-amylase inhibition, indicating promising anti-diabetic potential. Similar inhibitory effects have been reported for *Solanum* species and alginate-based herbal formulations. Although the activity was lower than metformin, the gradual increase with concentration suggests effective enzyme interaction. These findings align with previous reports highlighting the role of plant-derived compounds in managing post-prandial hyperglycemia [32].

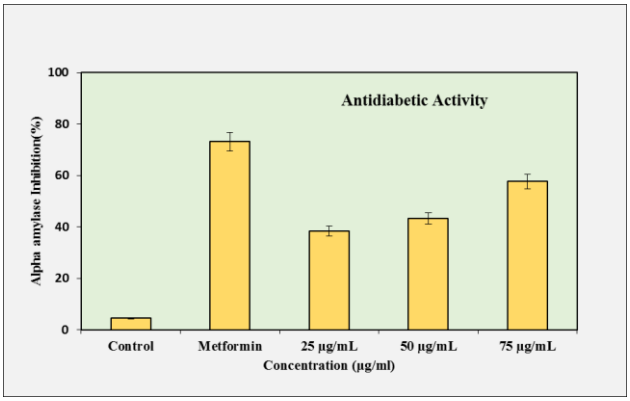

Fig 9 Alpha amylase inhibition shown by the *S. surattense* loaded OSA hydrogel at concentrations of 25 µg/mL, 50 µg/mL and 75 µg/mL compared with control and Metformin. The hydrogel displays a dose dependent increase in inhibition.

Anti-inflammatory Assay

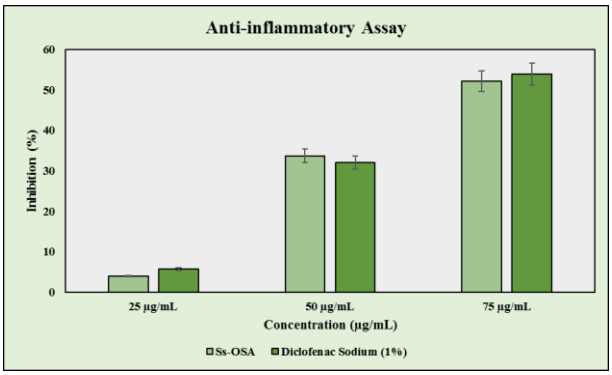

Fig 10. Anti-inflammatory activity of the sample at concentrations of 25 µg/mL, 50 µg/mL and 75 µg/mL compared with diclofenac sodium. The sample shows a steady dose dependent increase in inhibition and approaches the activity of the standard drug at the highest concentration.

The anti-inflammatory activity of the sample increases consistently with concentration. At 25 µg/mL, the inhibition is about 3.90%, which is slightly lower than diclofenac sodium at the same concentration, which shows 5.69%. This indicates only mild activity at the lowest level. At 50 µg/mL, the sample shows a clear rise to 33.65%, which is slightly higher than diclofenac sodium at 31.97%. This shows that the sample begins to

Journal of Chemical Health Risks

www.jchr.org

JCHR (2026) 16(2), 2005-2017 | ISSN:2251-6727

match the standard drug in activity at the mid concentration. At 75 µg/mL, the inhibition increases further to 52.19%, coming close to the diclofenac sodium value of 53.92% (**Fig** 10). This indicates that at higher concentrations the sample has strong anti-inflammatory potential and performs nearly equivalent to the standard. Overall, the results show a clear dose dependent improvement in anti-inflammatory behaviour. The anti-inflammatory activity of the Ss-OSA hydrogel increased significantly with concentration, approaching the efficacy of diclofenac sodium at higher doses. Comparable dose-dependent anti-inflammatory responses have been observed for alginate-encapsulated phytochemicals in earlier studies. The observed activity is likely due to the presence of bioactive compounds such as alkaloids and flavonoids in *Solanum surattense*. These results support previous findings that plant-based hydrogels can serve as effective anti-inflammatory therapeutic systems [33, 34].

4. Conclusion

The present study demonstrates that the oxidized sodium alginate (OSA) hydrogel loaded with *Solanum surattense* extract forms a stable, porous, and well-integrated polymeric network capable of supporting controlled bioactive delivery. Structural analyses confirmed successful chemical modification and effective incorporation of plant phytoconstituents within the alginate matrix. The porous surface morphology and predominantly amorphous structure contributed to a predictable biphasic release pattern, consisting of an initial burst followed by a sustained release phase. The hydrogel exhibited notable dose-dependent biological activities, including antioxidant, antidiabetic, and anti-inflammatory effects, highlighting the preserved bioactivity of the encapsulated extract. Cell-based assays further indicated that the material maintains favorable cellular compatibility while demonstrating therapeutic potential. Overall, the *S. surattense*-loaded OSA hydrogel represents a promising, biocompatible platform for controlled phytochemical delivery. Its multifunctional bioactivity and sustained release behavior make it a strong candidate for wound healing and related biomedical applications. These findings provide a foundation for further mechanistic investigations and future *in vivo* therapeutic studies.

Acknowledgments

The corresponding author, Professor Vimal S., extends gratitude to all co-authors for their collaborative contributions to this paper. This work was supported by the Department of Biochemistry, Saveetha Medical College and Hospital, Saveetha Institute of Medical and Technical Sciences (SIMATS), Thandalam, Chennai - 600 105, Tamil Nadu, India.

Data availability

The data supporting the findings of this study are available from the all authors request. All relevant data are included within the article and its supplementary materials.

Declarations

Ethical approval - Not required.

Competing interests

The authors declare no competing interests.

References

[1] Li, Ming, Wanying Zhao, Luyao Bai, et al. 2025. "Modulating Anti-Inflammatory Macrophage Polarization and Regulatory T Cell Differentiation via Aminooxyacetic Acid-Loaded Hydrogel for Promoting Allogeneic Skin Transplantation." *ACS Applied Bio Materials* 8 (12): 10979-10989.

[2] Lin, Ting-Shen, Ci-Wen Luo, Tsai-Ling Hsieh, Frank Cheau-Feng Lin, and Stella Chin-Shaw Tsai. 2024. "Transoral Robotic Surgery for Oral Cancer: Evaluating Surgical Outcomes in the Presence of Trismus." *Cancers* 16 (6). https://doi.org/10.3390/cancers16061111.

[3] Li, Yuxia, Junfeng Zhu, Lijun Chen, Ning Chen, Xiangli Chen, and Jiaxiang Lv. 2025. "Polysaccharide-Driven Self-Healing Dual-Network Hydrogel via Schiff Base for High-Performance Flexible Sensing." *Carbohydrate Polymers* 370 (December): 124404.

[4] Mitra, Ramkrishna, and Wei Jiang. 2022. *Decoding Non-Coding RNA Implicated in Cancer Cell Survival & Growth Modulation*. Frontiers Media SA.

[5] Motz, Kevin, Hsien-Yen Chang, Harry Quon, Jeremy Richmon, David W. Eisele, and Christine G. Gourin. 2017. "Association of Transoral

Journal of Chemical Health Risks

www.jchr.org

JCHR (2026) 16(2), 2005-2017 | ISSN:2251-6727

Robotic Surgery With Short-Term and Long-Term Outcomes and Costs of Care in Oropharyngeal Cancer Surgery." *JAMA Otolaryngology-- Head & Neck Surgery* 143 (6): 580-588.

[6] Muthusamy, Mudiyayirakkani, Pratibha Ramani, Paramasivam Arumugam, et al. 2025. "Assessment of Various Etiological Factors for Oral Squamous Cell Carcinoma in Non-Habit Patients- a Cross Sectional Case Control Study." *BMC Oral Health* 25 (1): 62.

[7] Nie, Lei, Qianqian Wei, Xiaoyue Ding, et al. 2025. "Schiff-Base Bioelectric and Bioactive Hydrogel Dressing Based on Chitosan, Alginate, and poly(N-Isopropylacrylamide) for Accelerating Wound Healing." *International Journal of Biological Macromolecules* 338 (Pt 1): 149474.

[8] Pan, Chang-Yo, Ting-Shen Lin, Tzu-Peng Lee, and Stella Chin-Shaw Tsai. 2025. "Transoral Robotic Surgery in Oral Tongue Cancer Patients with Trismus: A Retrospective Evaluation of Feasibility and Surgical Outcomes." *Oral Oncology* 168 (September): 107597.

[9] Poothakulath, Krishnan R., D. Pandiar, P. Ramani, S. Jayaraman, and R. Subramanian. 2023. "Comparison of Clinico-Demographic and Histological Parameters Between Young and Old Patients With Oral Squamous Cell Carcinoma." *Cureus* 15 (11). https://doi.org/10.7759/cureus.48137.

[10] Rajkumar, Rajamanickam. 2012. *Topics on Cervical Cancer With an Advocacy for Prevention*. BoD - Books on Demand.

[11] Rolland, George Z. 2007. *New Research on Cervical Cancer*. Nova Publishers.

[12] Skvortsova, Ira Ida, Elvira V. Grigorieva, Simona Kranjc Brezar, and Yue Zhao. 2023. *Cancer Cell Reprogramming: Impact on Carcinogenesis and Cancer Progression*. Frontiers Media SA.

[13] Tuerxun, Hatila, Jinqiu Li, Qian Liu, et al. 2025. "MICA/B-Driven NK Cell Dysfunction Promotes Cervical Cancer via Toll Signaling." *Experimental Cell Research*, December 29, 114876.

[14] United States. Congress. House. Committee on Commerce. Subcommittee on Health and the Environment. 1999. *Women's Health, Raising Awareness of Cervical Cancer: Hearing Before the Subcommittee on Health and Environment of the Committee on Commerce, House of Representatives, One Hundred Sixth Congress, First Session, March 16, 1999*.

[15] Varaj, Hector T. 2007. *Trends in Cervical Cancer Research*. Nova Publishers.

[16] Weinstein, Gregory S., Bert W. O'Malley Jr, J. Scott Magnuson, et al. 2012. "Transoral Robotic Surgery: A Multicenter Study to Assess Feasibility, Safety, and Surgical Margins." *The Laryngoscope* 122 (8): 1701-1707.

[17] Xu, Hongyan, Peng Zhang, Ying Yang, Jianhu Li, Jiaqiang Xu, and Tao Wang. 2025. "miRNA-337-3p and Matrix Metalloproteinase-9: Expression Patterns in Oral Squamous Cell Carcinoma and Prognostic Value for Cervical Lymph Node Metastasis." *Orthodontics & Craniofacial Research*, ahead of print, December 30. https://doi.org/10.1111/ocr.70093.

[18] Yu, Yee-Man, and 余綺雯. 2017. *Role of Amp-Activated Protein Kinase in Cervical Cancer Cell Growth*. Open Dissertation Press.

[19] Zhao, Yanwen, Yu Wang, Wenlong Sheng, et al. 2025. "A Multicomponent Salmon PDRN/Sodium Alginate/Gelatin Hydrogel Promotes Infected Wound Repair in Rat." *ACS Applied Bio Materials* 8 (12): 10742-10757.

[20] Zhu, Yi, Yiting Lou, Mengyuan Zhang, et al. 2026. "Histatin-1 Promotes Bone Regeneration by Coordinating Osteogenic and Angiogenic Responses in a Sustained-Release Hydrogel System." *Biomaterials Advances* 180 (March): 214618.

[21] Majeed M, Maqbool T, Majeed T, Arooj M, Danyaal S, Basirat A, Altaf A, Naz S, Muddassir M, Azhar MM. Anti-tumor and apoptotic potential of 4-hydroxy-2-methylbenzothiazole on MDA-MB-231 cell line. *[Journal Name]*. [Year];[Volume(Issue)]:[Page numbers].

[22] Sabbar AG, Mohsin AA. Synergistic anticancer and certain biochemical events impact ER+ MCF-7 breast cancer cells by local "Citrullus colocynthis-lemon fruit" hydroethanolic extract combination. *Asian Pac J Cancer Prev*. 2025;26(12):4617. doi:10.31557/APJCP.2025.26.12.4617.

Journal of Chemical Health Risks

www.jchr.org

JCHR (2026) 16(2), 2005-2017 | ISSN:2251-6727

[23] Dharmaraj, Kavya, and Reshma Poothakulath Krishnan. 2025. "Role of Tumor-Stroma Ratio in Oral Squamous Cell Carcinoma - A Cross-Sectional Study." *Bulletin of Stomatology and Maxillofacial Surgery* 21, no. 7: 284-289.

[24] Negahi A, Negahban H, Sayyad S, Khosravi-Mashizi M, Alijanpour A, Neamatzadeh H. Revolutionizing HER2-positive breast cancer treatment: insights from the 47th San Antonio Breast Cancer Symposium on trastuzumab deruxtecan. *Asian Pac J Cancer Prev*. 2025;26(8):2695. doi:10.31557/APJCP.2025.26.8.2695.

[25] Ragavendran C, Kamaraj C, Alrefaei AF, Priyadharsan A, de Matos LP, Malafaia G, .Moulishankar A, Thirugnanasambandam S. Green-route synthesis of ZnO nanoparticles via *Solanum surattense* leaf extract: Characterization, biomedical applications and ecotoxicity assessment of zebrafish embryo model. *South Afr J Bot*. 2024;167:643-662.

[26] Ragavendran C, Kamaraj C, Alrefaei AF, Priyadharsan A, de Matos LP, Malafaia G, Moulishankar A, Thirugnanasambandam S. Green-route synthesis of ZnO nanoparticles via *Solanum surattense* leaf extract: Characterization, biomedical applications and ecotoxicity assessment of zebrafish embryo model. *South Afr J Bot*. 2024;167:643-662.

[27] Bhoopathy J, Sathyaraj WV, Yesudhason BV, Rajendran S, Dharmalingam S, Seetharaman J, Muthu R, Murugesan R, Raghunandhakumar S, Anandasadagopan SK. Haemostatic potency of sodium alginate/aloe vera/sericin composite scaffolds: preparation, characterisation, and evaluation. *Biomater Sci*. 2023. doi:10.1080/21691401.2023.2293784. PMID: 38112317

[28] Balaji MB, *et al.* Fabrication and characterization of prednisolone-loaded *Bulletin of Material Sci*. 2024;47(1):148

[29] Dash, S. et al. (2010). Kinetic modeling on drug release from controlled drug delivery systems. *Journal of Controlled Release*, 147(1), 108 to 121. https://doi.org/10.1016/j.jconrel.2010.03.011

[30] Siepmann, J. and Peppas, N.A. (2001). Modeling of drug release from delivery systems based on hydroxypropyl methylcellulose. *Advanced Drug Delivery Reviews*, 48(2 to 3), 139 to 157. https://doi.org/10.1016/S0169-409X(01)00112-0

[31] Higuchi, T. (1963). Mechanism of sustained action medication. *Journal of Pharmaceutical Sciences*, 52(12), 1145 to 1149. https://doi.org/10.1002/jps.2600521210

[32] Peppas, N.A. et al. (2000). Physicochemical foundations and structural design of hydrogels in medicine and biology. *Annual Review of Biomedical Engineering*, 2, 9 to 29. https://doi.org/10.1146/annurev.bioeng.2.1.9

[33] George, M. and Abraham, T.E. (2006). Polyionic hydrocolloids for intestinal drug delivery. *Journal of Controlled Release*, 114(1), 1 to 14.

[34] Akshaya Viswanathan, Sajith S, Harini M, et al. Development of a *Calophyllum inophyllum*-Loaded Biodegradable Chitosan-PVA Hydrogel: A Multifunctional Platform for HT-29 Colon Cancer Cell, and Antidiabetic Applications. 2025.